THE JOURNAL OF BIOLOGICAL CHEMISTRY VOL. 288, NO. 5, pp. 2933–2940, February 1, 2013

Acute Mitochondrial Inhibition by Mitogen-activated Protein Kinase/Extracellular Signal-regulated Kinase Kinase (MEK) 1/2 Inhibitors Regulates Proliferation*

Received for publication, October 22, 2012, and in revised form, December 6, 2012 Published, JBC Papers in Press, December 12, 2012, DOI 10.1074/jbc.M112.430082

Maureen O. Ripple[1], **Namjoon Kim, and Roger Springett**

From the Department of Radiology, The Geisel School of Medicine at Dartmouth, Hanover, New Hampshire 03755

Background: Small molecule MEK1/2 inhibitors are designed to block ERK1/2-mediated signaling and inhibit proliferation.
Results: Novel instrumentation which measures cellular respiratory chain function found that four structurally distinct MEK1/2 inhibitors acutely affected mitochondrial bioenergetics.
Conclusion: The anti-mitochondrial effects of MEK1/2 inhibitors determined proliferative potential.
Significance: Impaired mitochondrial metabolism following MEK1/2 inhibition must be considered when using small molecule inhibitors to define this signaling pathway.

The Ras-MEK1/2-ERK1/2 kinase signaling pathway regulates proliferation, survival, and differentiation and, because it is often aberrant in tumors, is a popular target for small molecule inhibition. A novel metabolic analysis that measures the real-time oxidation state of NAD(H) and the hemes of the electron transport chain and oxygen consumption within intact, living cells found that structurally distinct MEK1/2 inhibitors had an immediate, dose-dependent effect on mitochondrial metabolism. The inhibitors U0126, MIIC and PD98059 caused NAD(H) reduction, heme oxidation, and decreased oxygen consumption, characteristic of complex I inhibition. PD198306, an orally active MEK1/2 inhibitor, acted as an uncoupler. Each MEK1/2 inhibitor depleted phosphorylated ERK1/2 and inhibited proliferation, but the most robust antiproliferative effects always correlated with the metabolic failure which followed mitochondrial inhibition rather than inhibition of MEK1/2. This warrants rethinking the role of ERK1/2 in proliferation and emphasizes the importance of mitochondrial function in this process.

Most cancers develop autonomy from growth factor signaling often through mutations or changes in protein expression (1). The mitogen-activated protein kinase (MAPK) cascades have been identified as key regulators of cellular proliferation, differentiation, and survival, and one of these cascades, Raf-MEK1/2-ERK1/2, has been the target of many pharmaceutical endeavors (2–7). Processes as diverse as survival following oxidant injury, steroid biosynthesis, VEGF release, neuronal development, and cell cycle progression are believed to be regulated via this cascade where the end point obtained depends not only on the phosphorylation event but also on factors such as the duration and cellular location of the signal (8–15).

Because RAS structural alterations occur in nearly 30% of all cancers and *BRAF* mutations have been found in up to 60% of certain cancers, small molecule inhibitors of this signaling pathway have been widely developed and tested (10, 16, 17). Several MEK1/2 inhibitors including selumetinib, MEK162, GSK1120212, CI-1040, PD0325901, and XL518 have either been or are currently being evaluated in phase I/II clinical trials, and still others are in preclinical development (3–5). The survival of many myeloid leukemia cells, both *in vitro* and *in vivo*, depends on the activation of this MAPK pathway, and various MEK1/2 inhibitors have been used to successfully inhibit leukemic proliferation (18, 19). In this study we tested four MEK1/2 inhibitors in HL-60 myeloid leukemia cells which harbor an N-*RAS* mutation and demonstrate constitutive MAPK activation (18, 20).

The most effective preclinical compounds targeting the Raf-MEK1/2-ERK1/2 pathway are against MEK1/2. Because ERK1/2 are the only known substrates of MEK1/2, the proliferative inhibition and reduced survival seen following MEK1/2 inhibition are attributed to ERK1/2-mediated factors (4, 7). PD98059 and U0126 are the most popular preclinical MEK1/2 inhibitors used to study this pathway, and the results obtained with these compounds in cell culture have been used to justify the development of clinical inhibitors. Here we show that these structurally distinct MEK1/2 inhibitors and a newer inhibitor, MEK inhibitor I (MIIC),[2] not only block ERK1/2 phosphorylation but also cause acute alterations of mitochondrial electron transport chain (ETC) function.

The ETC is composed of four protein complexes containing electron carriers embedded in the inner mitochondrial membrane and cytochrome *c* (Cyt*c*) present in the intermembrane space. Complex III, Cyt*c*, and cytochrome oxidase (complex IV) (CytOX) contain heme electron carriers which can either be oxidized (not carrying electrons) or reduced (carrying electrons), and their oxidation state can be measured with multi-wavelength cell spectroscopy. Inhibition of the mitochondrial complexes results in an upstream reduction and a downstream oxidation of the electron carriers as well as decreasing oxygen

* This work was supported, in whole or in part, by National Institutes of Health Grants 5R21RR25803 and R01NS054298.
[1] To whom correspondence should be addressed: Dept. of Radiology, The Geisel School of Medicine at Dartmouth, HB 7786, Hanover, NH 03755. Tel.: 603-650-1625; Fax: 603-650-1717; E-mail: maureen.ripple@dartmouth.edu.

[2] The abbreviations used are: MIIC, MEK inhibitor I; CCCP, carbonyl cyanide *m*-chlorophenylhydrazone; Cyt*c*, cytochrome *c*; CytOX, cytochrome oxidase; DMSO, dimethyl sulfoxide; ETC, electron transport chain.

consumption allowing multiwavelength cell spectroscopy, combined with NADH spectroscopy, to pinpoint the site of mitochondrial inhibition in living cells (21).

In this paper, we show that PD98059, U0126, and MIIC potently inhibit the ETC at complex I at concentrations routinely used in the literature for inhibition of MEK1/2, and we investigate the role of this inhibition on human leukemia cell proliferation. Furthermore, we show that PD198306, a newer and more potent MEK1/2 inhibitor, acts as a robust mitochondrial protonophore and uncouples oxidative phosphorylation at higher concentrations. In short, we show the strong mitochondrial effects of these compounds provide a new mechanism by which these inhibitors regulate cell proliferation.

EXPERIMENTAL PROCEDURES

Cell Culture—HL-60 cells were cultured at 37 °C in spinner flasks in phenol red-free RPMI 1640 medium (Invitrogen) containing antibiotic/antimycotic (Sigma) and 10% fetal bovine serum (Invitrogen) in a 95% air and 5% CO_2 incubator. Cell density and viability were determined via trypan blue exclusion using the Countess® Automated Cell Counter (Invitrogen). Proliferation was defined as the increase in viable (trypan blue-excluding) cells over time compared with vehicle control-treated cells. This definition takes into account changes due to cell division, differentiation, and death.

Inhibitors—U0126 ($C_{18}H_{16}N_6S_2$) and PD198306 ($C_{18}H_{16}F_3IN_2O_2$) were purchased from Tocris (Ellisville, MO). PD98059 ($C_{16}H_{13}NO_3$) was from Promega. MEK inhibitor I designated MIIC ($C_{21}H_{18}N_4OS$) was from EMD/Calbiochem. Rotenone and pyridaben were from Sigma. Rotenone was dissolved in ethanol. Pyridaben and the MEK1/2 inhibitors were dissolved in DMSO, and controls were treated with a correlating concentration of DMSO. Inhibitors were added as indicated in the figure legends.

Cell Spectroscopy and Analysis—Cells were spun down at 500 × *g* for 5 min and then resuspended in at a density of 2.0×10^7 cells/ml in RPMI 1640 medium and placed in a custom-built 5-ml chamber that consisted of a 17-mm inside-diameter quartz crucible embedded in an aluminum block maintained at 37.0 °C by a thermoelectric element. The oxygen concentration within the chamber was measured from the fluorescence lifetime of a phosphorescent membrane inserted through a 3-mm-diameter hole in the side of the crucible, and the top of the chamber was sealed with a stainless steel plunger. The stir bar was made of glass rather than Teflon, and all of the seals were made of Viton in accordance with good respirometry practice (22). The cells were oxygenated and deoxygenated under computer control by exchange of oxygen across 80 mm of oxygen-permeable silicone tubing immersed in the cell suspension using a feedback circuit to adjust the oxygen tension within the tubing to maintain constant oxygenation within the chamber; the tubing always contained 5% CO_2 to maintain intracellular pH. Oxygen consumption was measured from the difference between the oxygen delivery to the cell suspension by the tubing and the rate change of the oxygen concentration of the cell suspension. The oxygen delivery was calculated from the oxygen gradient across the wall of tubing and the oxygen permeability of the tubing which was measured prior to each study.

Spectroscopy and Spectral Analysis—Heme attenuation spectra and NADH fluorescence spectra were measured with two separate CCD-spectrograph systems working in time-multiplexed mode at 50 Hz using a 6-ms on/4-ms off duty cycle. Contiguous spectra were averaged to give a temporal resolution of 0.5 s. A warm white light emitting diode (LED) was used for the attenuation spectra illumination which was mounted 10 mm below a bundle of three NA0.37 1-mm optical fibers. One fiber was used for attenuation spectra detection, one for fluorescence spectra detection and one was coupled to a 365-nm UV LED for fluorescence excitation. The two detection fibers were F-matched onto the slits of two 0.3-mm spectrographs (Triax 320; Horiba, Edison, NJ), each equipped with a 1024 × 128-pixel back-thinned CCD camera (DV401BV; Andor Technology, South Windsor, CT). The attenuation spectrograph was equipped with a 600 g/mm grating blazed at 500 nm, which provided complete spectra between 508 and 640 nm with a pixel bandpass of 0.16 nm. The slits were set to give a spectral resolution of 1 nm. The NADH fluorescence spectrograph was equipped with a 300 g/mm grating blazed at 500 nm, which provided complete spectra between 400 and 670 nm with a pixel bandpass of 0.33 nm. The slits were set to give a spectral resolution of 20 nm.

Heme oxidation changes were calculated by fitting a linear combination of model spectra to the change in attenuation spectrum (23) over the wavelength range 520–630 nm. The model spectra were: b_H, b_L, c_1 hemes of complex III, Cyt*c*, a_{605}, a_{602}, and a_3 spectra from CytOx (23) and a quadratic background to account for any base-line drift. All model spectra were measured from the isolated enzymes except a_{602} (see Ref. 23). The b_{560} heme of complex II is not included in the model because it has a midpoint potential of −185mV (24) and so is unlikely to be reduced in the absence of exogenous reductants. The oxidized fraction of each heme (oxidation state) was calculated from the oxidation changes assuming full reduction during anoxia and full oxidation at high oxygen tension after addition of 1 μM complex I inhibitor rotenone.

NADH oxidation changes were calculated by fitting a linear combination of model spectra to the fluorescence intensity spectrum over the wavelength range 410–610 nm. The model spectra were the fluorescence spectrum of NADH, the fluorescence spectrum of the RPMI 1640 medium and a linear background. The NADH signal originates from both NADH and NADPH in both the cytosol and the mitochondria. The oxidation state of mitochondrial NADH was calculated from oxidation changes assuming full reduction of mitochondrial NADH during anoxia and full oxidation of mitochondrial NADH after 1 mM complex II inhibitor 3-nitropropionic acid, which inhibits the TCA cycle, and 1 μM protonophore carbonyl cyanide *m*-chlorophenyl hydrazone (CCCP), assuming that NADPH and cytosolic NADH did not change with these interventions.

Quantitative Western Blotting—Aliquots containing of 2.0×10^6 cells were removed from the chamber and immediately combined with 500 μl of cold PBS, centrifuged at 4.3 × *g* for 90 s, and the resulting pellet was resuspended in Laemmli buffer heated to 75 °C and heated for 5 min. The proteins were separated on a 14% SDS-polyacrylamide gel (Novex) and transferred to an Immobilon P membrane. Membranes were blocked in

Tris-buffered saline containing 0.05% Tween 20 (TBST) and 5% milk. Primary antibodies were diluted in TBST and 5% milk or BSA and exposed to the blot overnight at 4 °C. Primary antibodies ERK and phosphor-ERK (Thr-202, Tyr-204) were purchased from Cell Signaling. Blots were washed in TBST three times and exposed to fluorescent-conjugated secondary antibodies, mouse IgG IRDye800 (Rockland), and rabbit IgG Alexa Fluor 680, for 45 min. Blots were washed in TBST three times and once in TBS before being read on an Odyssey Imaging System (LiCor). Blots were analyzed and quantitated using custom software that corrects the fluorescence intensity of a protein band for the fluorescence intensity above and below the band. The amount of phosphorylated ERK1/2 fluorescence per total ERK1/2 fluorescence is expressed in the data, but it should be noted that this value is only proportional to the pERK1/2/total ERK1/2 due to differences in the efficiency of detection.

RESULTS

Dose-dependent Inhibition of Proliferation and Phosphorylation of ERK1/2 by Various MEK1/2 Inhibitors—MEK inhibitors slowed the proliferation of HL-60 cells in a dose-dependent manner that varied with inhibitor (Fig. 1*A*). Exponentially growing HL-60 cells were treated with 1 nM-300 μM inhibitor for 48 h, and the number of viable cells was calculated and related to the proliferation of vehicle (DMSO)-treated cells. PD198306 showed a slightly stronger inhibition of proliferation per dose than MIIC and U0126. All three of these drugs were more potent at inhibiting proliferation than PD98059, a first generation MEK1/2 inhibitor. A 50% inhibition of proliferation was detected with 300 μM PD98059, the highest concentration tested (Fig. 1*A*). U0126 and MIIC, at 30 μM, inhibited the proliferation of HL-60 cells by 67 and 77%, respectively. Phosphorylation of ERK1/2, the only known substrates of MEK1/2, is the standard assay of MEK1/2 activity. To determine the MEK1/2 activity of inhibitor-treated HL-60 cells, total cell extracts were made 2 min after exposure to 1–100 μM inhibitor. Western analysis indicated that little or no pERK1/2 was found following 1 μM MIIC, U0126, and PD198306 and 100 μM PD98059 (Fig. 1*B*).

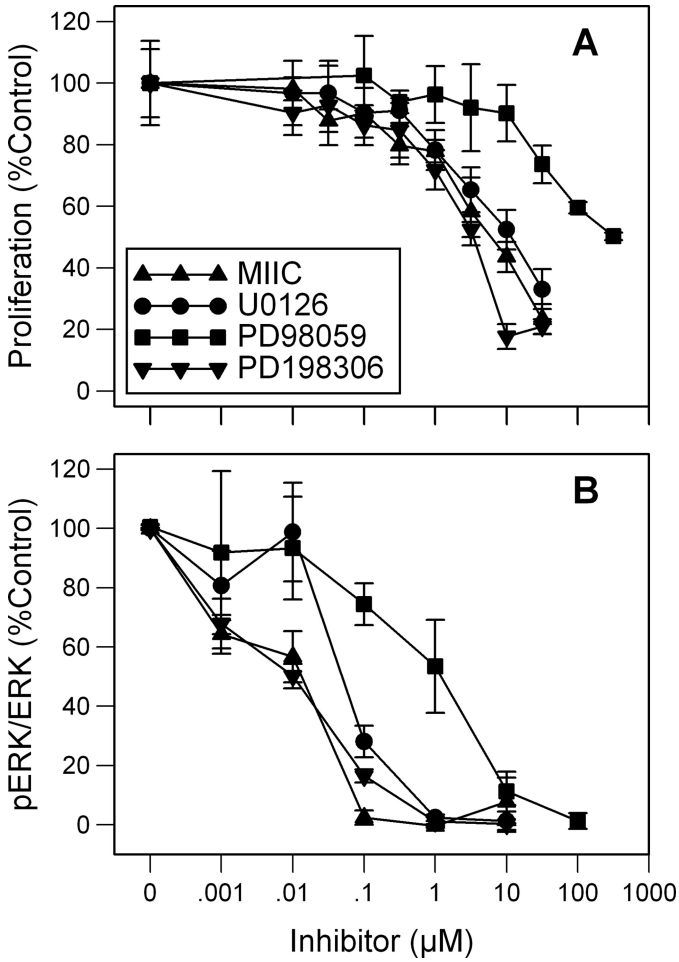

FIGURE 1. **Differential effects of MEK1/2 inhibitors on proliferation and pERK/ERK.** *A*, dose response of MIIC, U0126, PD98059, and PD19830 on proliferation and phosphorylated ERK1/2 per ERK1/2 is shown. *B*, HL-60 cells were incubated with 1 nM--300 μM inhibitor for 48 h. The number of live cells was determined by trypan blue exclusion, and results are expressed as a ratio of vehicle-control-treated cell proliferation (*A*). Differences are significantly less than control ($p < 0.05$) at concentrations of 0.1 μM PD198306, 0.3 μM MIIC, 1 μM U0126, and 30 μM PD98059 and greater. Phosphorylated ERK1/2 per total ERK1/2 was determined using Western blot analysis of lysates taken 2 min after exposure to 1 nM--100 μM inhibitor. Results are expressed as mean ± S.D. (*error bars*; $n = 3$) and are significantly less than base line ($p < 0.05$) at concentrations of 0.001 μM PD198306 and MIIC, 0.01 μM U0126, and 1 μM PD98059 and greater.

Direct Effects of MEK1/2 Inhibitors on the ETC and Evidence for Complex I Inhibition—Multiwavelength cell spectroscopy was used to quantitate oxidation changes of the ETC hemes simultaneously with oxygen consumption (VO_2). A typical study is shown in Fig. 2 where a downward deflection in Cyt*c* denotes reduction and an upward deflection denotes oxidation. Oxygen concentration within the chamber was maintained at 100 μM (~10% O_2) except in the *gray shaded area* where the O_2 concentration was altered under computer control. [O_2] was decreased to zero (anoxia) and maintained there for 2 min then returned to 100 μM. Under anoxic conditions, electrons are not able to leave the chain, and all of the upstream redox centers, including Cyt*c*, become fully reduced (Fig. 2, *A* and *B*). The addition of 1 μM rotenone, a complex I inhibitor, blocked entry of electrons into the chain, resulting in a complete oxidation of Cyt*c* and blocked all mitochondrial VO_2 (Fig. 2, *A* and *B*). The heme oxidation states were subsequently calculated assuming that the hemes were fully reduced and fully oxidized under anoxia and rotenone, respectively. The addition of U0126 indicated by the *arrows*, to final concentrations of 0.001, 0.003, 0.01, 0.03, 0.1, 0.3, 1, 3, 10, and 30 μM, resulted in a concentration-dependent decrease in VO_2 and oxidation of Cyt*c* (Fig. 2, *B* and *D*).

At base line 62 ± 1% of Cyt*c*, 69 ± 4% of b_H of the bc_1 complex (complex III) and 89 ± 3% of CytOx were oxidized (Fig. 3, *top*). DMSO, given as a vehicle control, slightly increased VO_2 but did not appreciably change the cytochrome oxidation state (Fig. 3, *left*). The addition of MIIC and U0126 caused a dose-dependent oxidation of Cyt*c*, b_H, and CytOx (Fig. 3, *top*). Cyt*c* was 97.5 ± 0.3% and 88.5 ± 0.2% oxidized after 10 μM MIIC and U0126, respectively, and nearly fully oxidized after 30 μM. The b_L and c_1 hemes of the bc_1 complex also oxidized in concert with the other hemes (data not shown). The oxidation was rapid and stabilized within 90 s (Fig. 2*D*). PD98059 also oxidized the hemes but required more drug, 30 μM and higher,

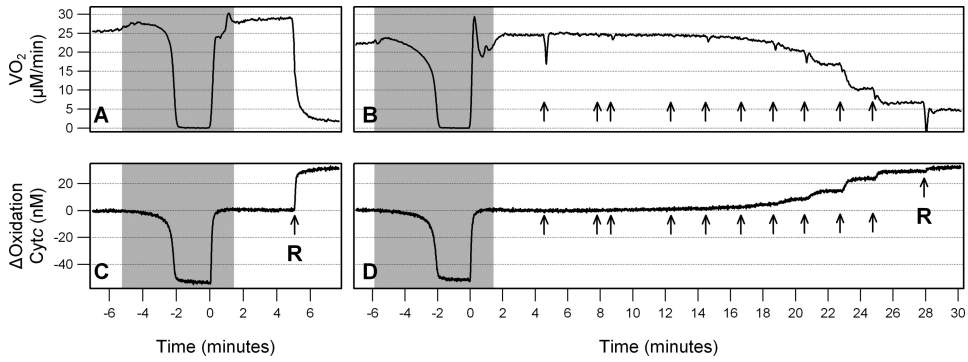

FIGURE 2. **U0126 acutely inhibits VO_2 and Cyt*c* oxidation in a concentration-dependent manner.** Representative data were obtained from the multiwavelength cell spectroscopy system. *Gray* denotes areas where [O_2] is <100 μM, and *arrows* show where inhibitor, either U0126 or 1 μM rotenone (*R*), was added. Oxygen consumption (VO_2) is shown in *A* and *B*. Change in Cyt*c* oxidation from base line is shown in *C* and *D*. *A* and *C* show a simple anoxia and rotenone study to fully reduce and fully oxidize the hemes. *B* and *D* show an anoxia, addition of U0126 to a final concentration of 0.001, 0.003, 0.01, 0.03, 0.1, 0.3, 1, 3, 10, and 30 μM, and finally rotenone.

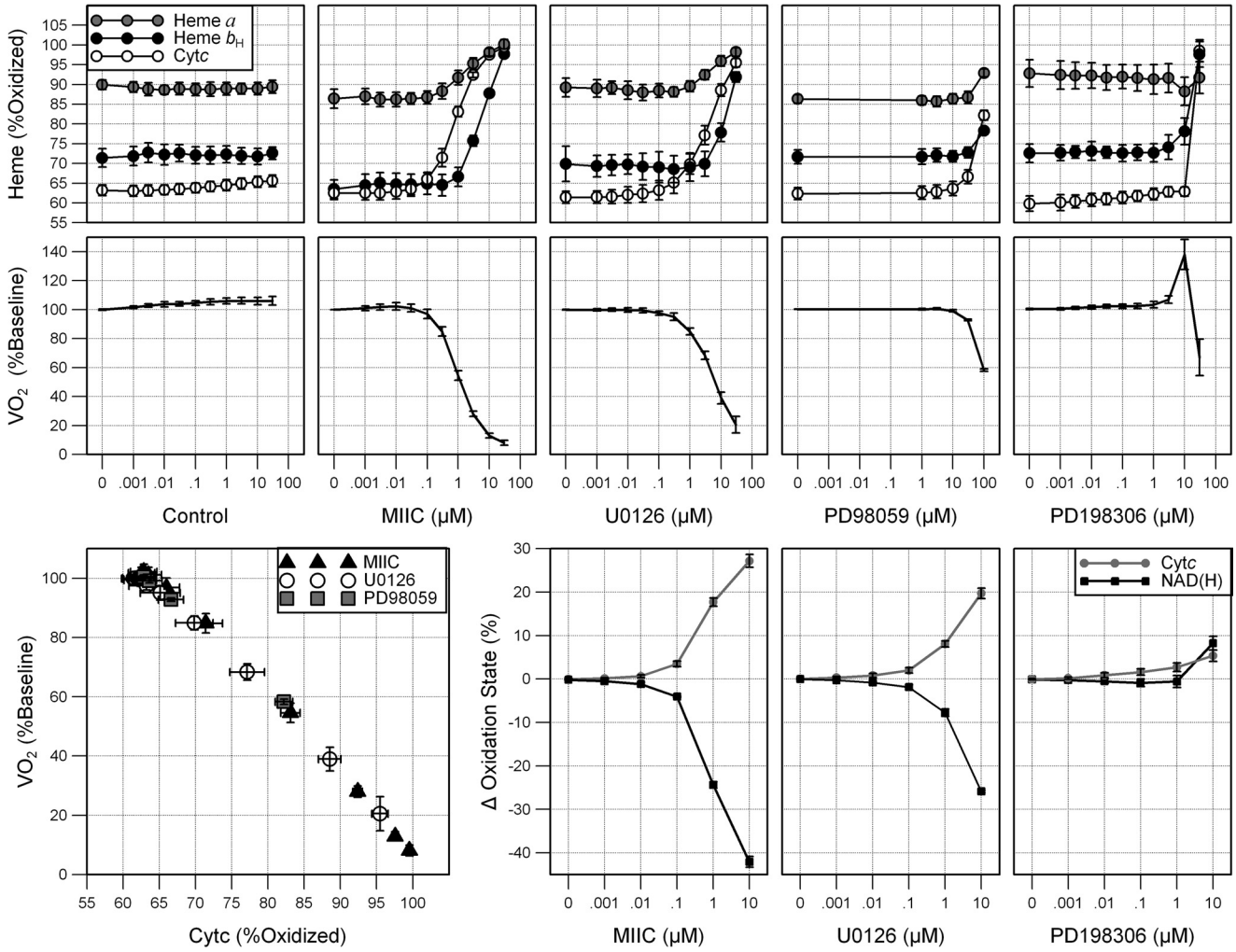

FIGURE 3. **Concentration-dependent inhibition of ETC by structurally distinct MEK1/2 inhibitors.** Oxidation state of heme b_H of complex III, Cyt*c*, and heme *a* of CytOx (*upper panels*), and oxygen consumption as a percentage of base line (*lower panels*) 2 min after treatment with 1 nM–30 μM MIIC, U0126, and PD198306, 1–100 μM PD98059, or equivalent amounts of vehicle-control (DMSO). Results are expressed as mean ± S.D. (*error bars*; $n = 6$). Cyt*c* changes were significant ($p < 0.005$) at concentrations of 0.03 μM and higher for MIIC and U0126 ($p < 0.05$) at and above 0.01 μM PD198306 and 3 μM PD98059. VO_2, CytOx, and Cytb_H changes were significant ($p < 0.05$), respectively, at the following concentrations: MIIC 0.3, 0.3, 1; U0126 0.1, 3, 10; PD98059 10, 100, 30; PD198306 0.03, 10, 10. Direct linear correlation between Cytc oxidation and VO_2 was found for MIIC, U0126, and PD98059. Cyt*c* oxidation and VO_2 were measured 2 min after treatment with varying doses of inhibitor. The linear regression for each inhibitor was $R2 > 0.99$. Changes in Cyt*c* oxidation state (*upper panels*) and NAD(H) oxidation state (*lower panels*) were measured following treatment with 0.001–10 μM MIIC, U0126, or PD198306. Measurements were taken 2 min after each dose. Results are expressed as mean ± S.D. ($n = 3$). $p < 0.01$ at concentrations of 1 μM U0126, 0.1 μM MIIC, and 10 μM PD198306 and higher.

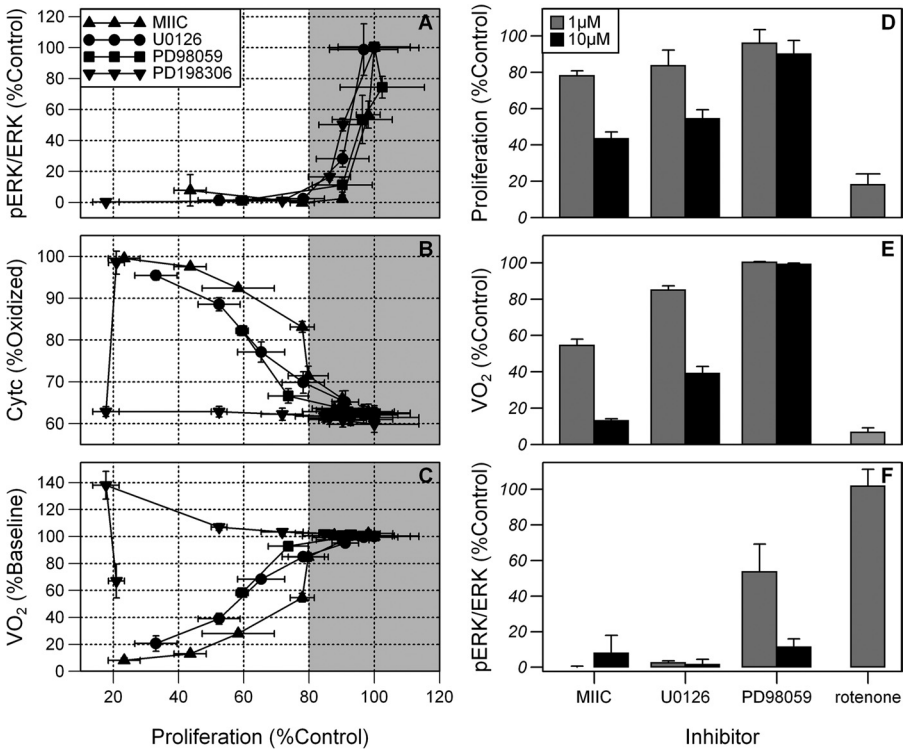

FIGURE 4. **Antiproliferative effects of MEK1/2 inhibitors depend on mitochondrial inhibition.** *A–C*, fraction of control proliferation *versus* the loss of pERK1/2/ERK1/2 (*A*), Cytc oxidation state (*B*), and VO_2 (*C*) in HL-60 cells. Measurements of Cytc and VO_2 were taken 2 min after each dose and are expressed as mean ± S.D. (*error bars*; $n = 6$) and cell lysates were obtained for pERK1/2 and ERK1/2 determination after 5 min and are expressed as mean ± S.D. ($n = 3$). MIIC, U0126, and PD198306 were used at concentrations of 0.001–30 μM and PD98059 at 0.001–100 μM. *D–F*, comparison of the effects of 1 μM and 10 μM MIIC, U0126, PD98059, and 1 μM rotenone on proliferation (*D*), VO_2 (*E*), and pERK1/2/ERK1/2 expression (*F*) relative to control. Proliferation was measured at 48 h and VO_2, and pERK1/2/ERK1/2 expression was measured at 2 and 5 min, respectively.

to do so. PD198306, a newer generation MEK1/2 inhibitor, had little effect on the heme oxidation state until the highest concentration, 30 μM. A dose-dependent decrease in VO_2 was noted following treatment with MIIC or U0126 (Fig. 3, *bottom*). Similarly, PD98059 decreased VO_2 but required a greater concentration of drug. In contrast, PD198306 first increased VO_2 at moderate concentrations (3 and 10 μM) and then decreased VO_2 at the highest concentration (30 μM), where it also oxidized Cyt*c* and b_H. U0124, sold as a small molecule control for U0126 studies, had no effect VO_2 or cytochrome oxidation state (data not shown).

A direct linear correlation, $R>0.99$, between Cyt*c* oxidation and VO_2 was found for MIIC, U0126, and PD98059 (Fig. 3, *lower left*). As each of these compounds was added Cyt*c* oxidation increased in concert with a decrease in VO_2. The results suggest that these inhibitors have the same mechanism of action on the mitochondria.

The oxidation of all ETC hemes along with inhibition of VO_2 indicated that the MEK1/2 inhibitors were disrupting the ETC upstream of complex III. Similar to the hemes, NAD^+ and NADH are a redox couple where NADH is the reduced form (carrying two electrons) and NAD^+ is the oxidized form. To determine whether the inhibition was occurring at complex I or upstream of complex I, the oxidation state of NAD(H) was measured fluorometrically. Treatment with MIIC and U0126 resulted in a concentration-dependent reduction in NAD(H) which was significant starting at 0.1 μM and 1 μM ($p < 0.005$), respectively (Fig. 3, *lower right*). The effect of PD98059 could not be determined because the drug itself fluoresced. U0126 also fluoresced, but it could be spectrally resolved. PD198306 resulted in an oxidation in NAD(H) at 10 μM.

Complex I and Proliferative Inhibition Independent of MEK1/2 Inhibition—The concentration of each inhibitor required to reduce phosphorylation of ERK1/2 to ≤5% of base line produced only a 10–25% decrease in proliferation compared with vehicle-treated control cells at 48 h (Fig. 4*A*, *gray section*). Improved proliferative inhibition to 80% of control occurred at higher doses, with little or no further decrease in pERK1/2 levels. For the inhibitors MIIC, U0126, and PD98059 this improved proliferative inhibition strongly correlated with the oxidation of Cyt*c* and a decrease in VO_2 (Fig. 4, *B* and *C*). These changes are indicative of inhibition of the ETC. Similarly, PD198306 inhibits proliferation by just 25% when pERK1/2 is <5% of control. A greater proliferative inhibition was noted at higher doses, which did not decrease pERK1/2 levels further but did alter mitochondrial function.

Rotenone, an established complex I inhibitor, caused no decrease in pERK1/2/ERK1/2 although there was significant inhibition of proliferation at 48 h to 18 ± 6% of vehicle-treated control cells, suggesting loss of pERK1/2 is not necessary for complex I inhibition (Fig. 4, *D* and *F*). As expected, 1 μM rotenone fully oxidized Cyt*c* and inhibited VO_2 to 6.2 ± 2.4% of control; the residual VO_2 was nonmitochondrial in origin (Fig. 4*E*). Another known complex I inhibitor, pyridaben (1 μM), also oxidized Cyt*c*, abolished mitochondrial VO_2, and inhibited

proliferation to 44 ± 4% of control (data not shown), showing that complex I inhibition robustly affects proliferation.

At 1 μM, MIIC and U0126 had only modest effects on proliferation despite lowering pERK1/2/ERK1/2 to <2.5% of control levels. This concentration caused partial inhibition of complex I as indicated by the intermediate inhibition of VO_2 and oxidation of ETC cytochromes (Figs. 4*E* and 3). At a higher concentration of 10 μM, MIIC and U0126 further decreased VO_2 and further inhibited proliferation but caused no detectable change in pERK1/2/ERK1/2 (Fig. 4, *D–F*), suggesting that the robust inhibition of proliferation is dependent on complex I inhibition. In contrast, the MEK1/2 inhibitor PD98059 at 10 μM inhibited pERK1/2/ERK1/2 to 11.3 ± 4.6% of control but had little effect on VO_2, Cyt*c* oxidation, or on proliferation, again suggesting that lowering pERK1/2/ERK1/2 alone has little effect on proliferation. Together these data support the requirement of complex I activity over pERK1/2 expression for maintenance of proliferation.

DISCUSSION

Using a new technology that provides a real-time depiction of mitochondrial metabolism in intact cells via measurements of NAD(H) oxidation state, heme oxidation states, and oxygen consumption, we found that several structurally distinct MEK1/2 inhibitors acutely and effectively altered mitochondrial metabolism. Three of the inhibitors tested, U0126, MIIC, and PD98059, had dose-dependent immediate effects on complex I of the ETC. Another MEK1/2 inhibitor, PD198306, acted acutely as a protonophore. As expected, all of the MEK1/2 inhibitors blocked phosphorylation of ERK1/2 in a dose-dependent manner, and all slowed the proliferation of HL-60 human leukemia cells. Notably, the depletion of pERK1/2 to levels <5% of control correlated with just a 10–25% decrease in proliferation compared with control. Further proliferative inhibition, down to 80% of control, occurred at higher doses of inhibitor and correlated strongly with the effects on the mitochondrial electron transport.

The immediate, dose-dependent reduction in NAD(H) and oxidation in heme b_H of complex III, Cyt*c*, and heme *a* of CytOx, as well as the corresponding decrease in VO_2 caused by MIIC, U0126, and PD98059 are hallmarks of complex I inhibition. Such inhibition would explain the increase in the ADP:ATP ratio found in HEK293 cells treated with U0126 and PD98059 (25). U0126 also caused Cyt*c* oxidation and inhibited VO_2 in a normal mouse macrophage cell line, RAW264.7, and in two other human myeloid leukemia cell lines, ML-1 and AML-3 (data not shown), indicating that the inhibition of complex I is not specific to HL-60 cells. In addition, we found that U0126 oxidized Cyt*c* and inhibited VO_2 in isolated HL-60 mitochondria (data not shown), suggesting that U0126 acts to inhibit complex I independently of cytoplasmic MEK1/2. At least 60 different families of compounds have been found to inhibit complex I, highlighting its sensitivity to a vast variety of structurally unrelated natural and artificial compounds (26). The oxidation of Cyt*c* in HL-60 cells was maintained for at least 2 days following a single dose of U0126 (data not shown), suggesting that the inhibition is prolonged.

It is possible that the structurally distinct inhibitors U0126, MIIC, and PD98059 bind directly to complex I. Alternatively, inhibition could be occurring through a signaling event. Such a signaling cascade would require a terminal signaling protein with access to complex I and therefore present in either the mitochondrial intermembrane space or the mitochondrial matrix. There have been several reports of the presence of ERK1/2 in mitochondria, but it is difficult to reconcile the mitochondrial location of ERK1/2 with the impermeability of the outer mitochondrial membrane to proteins lacking a mitochondrial import sequence (27–29). In any case, inhibition of complex I by MEK1/2 or ERK1/2 can be ruled out because low dose PD198306 resulted in the profound loss of pERK1/2, presumably indicating complete inhibition of MEK1/2 kinase activity, with no observable inhibition of complex I. Kinase inhibitors are notoriously nonspecific, and it remains possible that these compounds are targeting a kinase within the mitochondria whose physiological substrate is complex I. The mammalian complex I contains 45 subunits (30), and some of the subunits reportedly contain phosphorylation sites (31, 32) although consensus has not been reached as to their functionality and relevance (33).

Low concentrations of a protonophore decrease the membrane potential and stimulate respiration whereas high concentrations cause a decrease in respiration concomitant with a failure in the TCA cycle to reduce NADH (34). Our previous work with the protonophore CCCP has shown the Cyt*c* oxidation state changes very little at low concentrations, where VO_2 increases, but becomes highly oxidized at higher concentrations where VO_2 decreases (35). PD198306 produced exactly this pattern of oxidation and electron flux changes consistent with it acting as a protonophore. Increases in VO_2 can also arise if ATP consumption is increased, but the changes observed with PD198306 also occurred in the presence of the ATP synthase inhibitor oligomycin, indicating that ATP consumption is not driving the increased VO_2 (data not shown). Similar to CCCP and another protonophore, carbonyl cyanide *p*-trifluoromethoxyphenylhydrazone (FCCP), PD198306 contains a secondary amine group which, in this case, bridges two benzene rings. Loss of the proton on the amine group would lead to a negative charge that would be delocalized over the two benzene rings, thus explaining the protonophore activity at higher concentrations. It should be noted that PD198306 is a structural analog of the MEK1/2 inhibitors, CI-1040 and MEK162, used in clinical trials.

In summary, the role of the MAPK signaling pathway in cellular proliferation is well established, and the overexpression or activation of the upstream components of this pathway in certain cancers is undeniable; however, the use of MEK1/2-specific inhibitors to define the function of this pathway must be accepted with caution. As we have clearly shown, MEK1/2 inhibitors of diverse structure can alter mitochondrial metabolism in addition to depleting pERK1/2. Because the reduction of pERK1/2 to <5% of base line corresponded to only a 10–25% decrease in proliferation compared with control regardless of the inhibitor used and because the mitochondrial inhibition continued to correlate with enhanced proliferative inhibition, we propose a prominent role for mitochondrial-mediated pro-

liferative control by these inhibitors. The concentrations used to obtain this level of proliferative inhibition were consistent with those published in the majority of literature related to these MEK1/2 inhibitors (36–41). Therefore, it is likely that many of the antiproliferative effects associated with these inhibitors are due to inhibition of mitochondrial function rather than strictly being mediated by the loss of pERK1/2.

REFERENCES

1. Hanahan, D., and Weinberg, R. A. (2000) The hallmarks of cancer. *Cell* **100,** 57–70
2. Shaw, R. J., and Cantley, L. C. (2006) Ras, PI(3)K and mTOR signalling control tumour cell growth. *Nature* **441,** 424–430
3. Frémin, C., and Meloche, S. (2010) From basic research to clinical development of MEK1/2 inhibitors for cancer therapy. *J. Hematol. Oncol.* **3,** 8
4. Roberts, P. J., and Der, C. J. (2007) Targeting the Raf-MEK-ERK mitogen-activated protein kinase cascade for the treatment of cancer. *Oncogene* **26,** 3291–3310
5. Sebolt-Leopold, J. S. (2008) Advances in the development of cancer therapeutics directed against the RAS-mitogen-activated protein kinase pathway. *Clin. Cancer Res.* **14,** 3651–3656
6. Pagès, G., Lenormand, P., L'Allemain, G., Chambard, J. C., Meloche, S., and Pouysségur, J. (1993) Mitogen-activated protein kinases p42MAPK and p44 MAPK are required for fibroblast proliferation. *Proc. Natl. Acad. Sci. U.S.A.* **90,** 8319–8323
7. Osborne, J. K., Zaganjor, E., and Cobb, M. H. (2012) Signal control through Raf: in sickness and in health. *Cell Res.* **22,** 14–22
8. Paz, C., Poderoso, C., Maloberti, P., Cornejo Maciel, F., Mendez, C., Poderoso, J. J., and Podestá, E. J. (2009) Detection of a mitochondrial kinase complex that mediates PKA-MEK-ERK-dependent phosphorylation of mitochondrial proteins involved in the regulation of steroid biosynthesis. *Methods Enzymol.* **457,** 169–192
9. Liu, X., Yan, S., Zhou, T., Terada, Y., and Erikson, R. L. (2004) The MAP kinase pathway is required for entry into mitosis and cell survival. *Oncogene* **23,** 763–776
10. Steelman, L. S., Franklin, R. A., Abrams, S. L., Chappell, W., Kempf, C. R., Bäsecke, J., Stivala, F., Donia, M., Fagone, P., Nicoletti, F., Libra, M., Ruvolo, P., Ruvolo, V., Evangelisti, C., Martelli, A. M., and McCubrey, J. A. (2011) Roles of the Ras/Raf/MEK/ERK pathway in leukemia therapy. *Leukemia* **25,** 1080–1094
11. Berra, E., Pagès, G., and Pouysségur, J. (2000) MAP kinases and hypoxia in the control of VEGF expression. *Cancer Metastasis Rev.* **19,** 139–145
12. Meloche, S., and Pouysségur, J. (2007) The ERK1/2 mitogen-activated protein kinase pathway as a master regulator of the G_1 to S phase transition. *Oncogene* **26,** 3227–3239
13. Klesse, L. J., Meyers, K. A., Marshall, C. J., and Parada, L. F. (1999) Nerve growth factor induces survival and differentiation through two distinct signaling cascades in PC12 cells. *Oncogene* **18,** 2055–2068
14. Newbern, J. M., Li, X., Shoemaker, S. E., Zhou, J., Zhong, J., Wu, Y., Bonder, D., Hollenback, S., Coppola, G., Geschwind, D. H., Landreth, G. E., and Snider, W. D. (2011) Specific functions for ERK/MAPK signaling during PNS development. *Neuron* **69,** 91–105
15. Guyton, K. Z., Liu, Y., Gorospe, M., Xu, Q., and Holbrook, N. J. (1996) Activation of mitogen-activated protein kinase by H2O2. Role in cell survival following oxidant injury. *J. Biol. Chem.* **271,** 4138–4142
16. Davies, H., Bignell, G. R., Cox, C., Stephens, P., Edkins, S., Clegg, S., Teague, J., Woffendin, H., Garnett, M. J., Bottomley, W., Davis, N., Dicks, E., Ewing, R., Floyd, Y., Gray, K., Hall, S., Hawes, R., Hughes, J., Kosmidou, V., Menzies, A., Mould, C., Parker, A., Stevens, C., Watt, S., Hooper, S., Wilson, R., Jayatilake, H., Gusterson, B. A., Cooper, C., Shipley, J., Hargrave, D., Pritchard-Jones, K., Maitland, N., Chenevix-Trench, G., Riggins, G. J., Bigner, D. D., Palmieri, G., Cossu, A., Flanagan, A., Nicholson, A., Ho, J. W., Leung, S. Y., Yuen, S. T., Weber, B. L., Seigler, H. F., Darrow, T. L., Paterson, H., Marais, R., Marshall, C. J., Wooster, R., Stratton, M. R., and Futreal, P. A. (2002) Mutations of the *BRAF* gene in human cancer. *Nature* **417,** 949–954
17. Brose, M. S., Volpe, P., Feldman, M., Kumar, M., Rishi, I., Gerrero, R., Einhorn, E., Herlyn, M., Minna, J., Nicholson, A., Roth, J. A., Albelda, S. M., Davies, H., Cox, C., Brignell, G., Stephens, P., Futreal, P. A., Wooster, R., Stratton, M. R., and Weber, B. L. (2002) *BRAF* and *RAS* mutations in human lung cancer and melanoma. *Cancer Res.* **62,** 6997–7000
18. Morgan, M. A., Dolp, O., and Reuter, C. W. (2001) Cell-cycle-dependent activation of mitogen-activated protein kinase kinase (MEK1/2) in myeloid leukemia cell lines and induction of growth inhibition and apoptosis by inhibitors of RAS signaling. *Blood* **97,** 1823–1834
19. Milella, M., Kornblau, S. M., Estrov, Z., Carter, B. Z., Lapillonne, H., Harris, D., Konopleva, M., Zhao, S., Estey, E., and Andreeff, M. (2001) Therapeutic targeting of the MEK/MAPK signal transduction module in acute myeloid leukemia. *J. Clin. Invest.* **108,** 851–859
20. Collins, S. J. (1987) The HL-60 promyelocytic leukemia cell line: proliferation, differentiation, and cellular oncogene expression. *Blood* **70,** 1233–1244
21. Hollis, V. S., Palacios-Callender, M., Springett, R. J., Delpy, D. T., and Moncada, S. (2003) Monitoring cytochrome redox changes in the mitochondria of intact cells using multi-wavelength visible light spectroscopy. *Biochim. Biophys. Acta* **1607,** 191–202
22. Haller, T., Ortner, M., and Gnaiger, E. (1994) A respirometer for investigating oxidative cell metabolism: toward optimization of respiratory studies. *Anal. Biochem.* **218,** 338–342
23. Kim, N., Ripple, M. O., and Springett, R. (2011) Spectral components of the α-band of cytochrome oxidase. *Biochim. Biophys. Acta* **1807,** 779–787
24. Yu, L., Xu, J. X., Haley, P. E., and Yu, C. A. (1987) Properties of bovine heart mitochondrial cytochrome b_{560}. *J. Biol. Chem.* **262,** 1137–1143
25. Dokladda, K., Green, K. A., Pan, D. A., and Hardie, D. G. (2005) PD98059 and U0126 activate AMP-activated protein kinase by increasing the cellular AMP:ATP ratio and not via inhibition of the MAP kinase pathway. *FEBS Lett.* **579,** 236–240
26. Degli Esposti, M. (1998) Inhibitors of NADH-ubiquinone reductase: an overview. *Biochim. Biophys. Acta* **1364,** 222–235
27. Wortzel, I., and Seger, R. (2011) The ERK cascade: distinct functions within various subcellular organelles. *Genes Cancer* **2,** 195–209
28. Nowak, G., Clifton, G. L., Godwin, M. L., and Bakajsova, D. (2006) Activation of ERK1/2 pathway mediates oxidant-induced decreases in mitochondrial function in renal cells. *Am. J. Physiol. Renal. Physiol.* **291,** F840–855
29. Becker, T., Böttinger, L., and Pfanner, N. (2012) Mitochondrial protein import: from transport pathways to an integrated network. *Trends Biochem. Sci.* **37,** 85–91
30. Efremov, R. G., Baradaran, R., and Sazanov, L. A. (2010) The architecture of respiratory complex I. *Nature* **465,** 441–445
31. Papa, S., Sardanelli, A. M., Scacco, S., Petruzzella, V., Technikova-Dobrova, Z., Vergari, R., and Signorile, A. (2002) The NADH: ubiquinone oxidoreductase (complex I) of the mammalian respiratory chain and the cAMP cascade. *J. Bioenerg. Biomembr.* **34,** 1–10
32. Chen, R., Fearnley, I. M., Peak-Chew, S. Y., and Walker, J. E. (2004) The phosphorylation of subunits of complex I from bovine heart mitochondria. *J. Biol. Chem.* **279,** 26036–26045
33. Schilling, B., Bharath, M. M. S., Row, R. H., Murray, J., Cusack, M. P., Capaldi, R. A., Freed, C. R., Prasad, K. N., Andersen, J. K., and Gibson, B. W. (2005) Rapid purification and mass spectrometric characterization of mitochondrial NADH dehydrogenase (complex I) from rodent brain and a dopaminergic neuronal cell line. *Mol. Cell. Proteomics.* **4,** 84–96
34. Steinlechner-Maran, R., Eberl, T., Kunc, M., Margreiter, R., and Gnaiger, E. (1996) Oxygen dependence of respiration in coupled and uncoupled endothelial cells. *Am. J. Physiol.* **271,** C2053–2061
35. Kim, N., Ripple, M. O., and Springett, R. (2012) Measurement of the mitochondrial membrane potential and pH gradient from the redox Poise of the hemes of the bc_1 complex. *Biophys. J.* **102,** 1194–1203
36. Ripple, M. O., Kalmadi, S., and Eastman, A. (2005) Inhibition of either phosphatidylinositol 3-kinase/Akt or the mitogen/extracellular-regulated kinase, MEK/ERK, signaling pathways suppress growth of breast cancer cell lines, but MEK/ERK signaling is critical for cell survival. *Breast Cancer Res. Treat.* **93,** 177–188
37. DeSilva, D. R., Jones, E. A., Favata, M. F., Jaffee, B. D., Magolda, R. L., Trzaskos, J. M., and Scherle, P. A. (1998) Inhibition of mitogen-activated

protein kinase kinase blocks T cell proliferation but does not induce or prevent anergy. *J. Immunol.* **160,** 4175–4181
38. Bost, F., McKay, R., Dean, N., and Mercola, D. (1997) The JUN kinase/stress-activated protein kinase pathway is required for epidermal growth factor stimulation of growth of human A549 lung carcinoma cells. *J. Biol. Chem.* **272,** 33422–33429
39. Hotokezaka, H., Sakai, E., Kanaoka, K., Saito, K., Matsuo, K., Kitaura, H., Yoshida, N., and Nakayama, K. (2002) U0126 and PD98059, specific inhibitors of MEK, accelerate differentiation of RAW264.7 cells into osteoclast-like cells. *J. Biol. Chem.* **277,** 47366–47372
40. Gysin, S., Lee, S. H., Dean, N. M., and McMahon, M. (2005) Pharmacologic inhibition of RAF→MEK→ERK signaling elicits pancreatic cancer cell cycle arrest through induced expression of $p27^{Kip1}$. *Cancer Res.* **65,** 4870–4880
41. Beloueche-Babari, M., Jackson, L. E., Al-Saffar, N. M., Workman, P., Leach, M. O., and Ronen, S. M. (2005) Magnetic resonance spectroscopy monitoring of mitogen-activated protein kinase signaling inhibition. *Cancer Res.* **65,** 3356–3363